Crystal Structure of Serine Dehydratase from Rat Liver[†,‡]

Taro Yamada,[§] Junichi Komoto,[§] Yoshimi Takata,[§,||] Hirofumi Ogawa,[||] Henry C. Pitot,[⊥] and Fusao Takusagawa*[,§]

Department of Molecular Biosciences, University of Kansas, 1200 Sunnyside Avenue, Lawrence, Kansas 66045-7534, Department of Biochemistry, Faculty of Medicine, Toyama Medical and Pharmaceutical University, Sugitani, Toyama 930-0194, Japan, and McArdle Laboratory for Cancer Research, University of Wisconsin Medical School, Madison, Wisconsin 53706-1599

Received July 24, 2003; Revised Manuscript Received September 7, 2003

ABSTRACT: SDH (L-serine dehydratase, EC 4.3.1.17) catalyzes the pyridoxal 5′-phosphate (PLP)-dependent dehydration of L-serine to yield pyruvate and ammonia. Liver SDH plays an important role in gluconeogenesis. Formation of pyruvate by SDH is a two-step reaction in which the hydroxyl group of serine is cleaved to produce aminoacrylate, and then the aminoacrylate is deaminated by nonenzymatic hydrolysis to produce pyruvate. The crystal structure of rat liver apo-SDH was determined by single isomorphous replacement at 2.8 Å resolution. The holo-SDH crystallized with *O*-methylserine (OMS) was also determined at 2.6 Å resolution by molecular replacement. SDH is composed of two domains, and each domain has a typical $\alpha\beta$-open structure. The active site is located in the cleft between the two domains. The holo-SDH contained PLP−OMS aldimine in the active site, indicating that OMS can form the Schiff base linkage with PLP, but the subsequent dehydration did not occur. Apo-SDH forms a dimer by inserting the small domain into the catalytic cleft of the partner subunit so that the active site is closed. Holo-SDH also forms a dimer by making contacts at the back of the clefts so that the dimerization does not close the catalytic cleft. The phosphate group of PLP is surrounded by a characteristic G-rich sequence (^{168}GGGGL^{172}) and forms hydrogen bonds with the amide groups of those amino acid residues, suggesting that the phosphate group can be protonated. N_1 of PLP participates in a hydrogen bond with Cys303, and similar hydrogen bonds with N_1 participating are seen in other β-elimination enzymes. These hydrogen bonding schemes indicate that N_1 is not protonated, and thus, the pyridine ring cannot take a quinone-like structure. These characteristics of the bound PLP suggest that SDH catalysis is not facilitated by forming the resonance-stabilized structure of the PLP−Ser aldimine as seen in aminotransferases. A possible catalytic mechanism involves the phosphate group, surrounded by the characteristic sequence, acting as a general acid to donate a proton to the leaving hydroxyl group of serine.

SDH[1] (L-serine dehydratase, EC 4.3.1.17) catalyzes the pyridoxal phosphate (PLP)-dependent dehydration of L-serine to yield pyruvate and ammonia (*1*). Rat liver SDH plays an important role in gluconeogenesis because the enzyme activity is induced remarkably by the consumption of high-protein diets, starvation, and other treatments (*2*). Formation of pyruvate by SDH is two-step reaction in which the hydroxyl group of serine is cleaved to produce aminoacrylate, and then the aminoacrylate is deaminated by nonenzymatic hydrolysis to produce pyruvate, giving the overall reaction shown below (*3*).

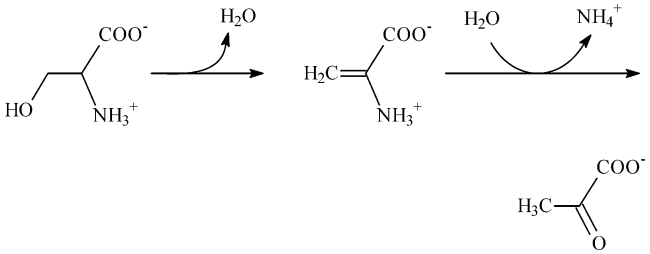

PLP-dependent enzymes are classified into at least three families (α, β, and γ) on the basis of their primary sequences (*4*). SDH, which catalyzes α,β-elimination, belongs to the β-family. The other members of this family include tryptophan synthase and *O*-acetylserine sulfhydrylase (*4*). In microorganisms, such as *Escherichia* and *Saccharomyces*, and in plants, there are often two isozymes of SDHs: one involved in the biodegradative pathway of serine (and threonine) and the other involved in the isoleucine biosynthesis pathway when the microorganisms are cultured in minimal medium. These SDHs are all composed of four identical subunits with an M_r in the range of 35200−63800 and are subject to allosteric regulation with AMP as an activator and isoleucine as an inhibitor (*5*, *6*).

Rat liver contains a relatively high concentration of SDH among the mammalian livers examined so far, and the

[†] This work was supported by NIH Grant GM37233.

[‡] The atomic coordinates of apo-SDH and SDH−(OMS−PLP) have been deposited with the Protein Data Bank as entries 1PWE and 1PWH, respectively. The amino acid sequence in the GenBank was adopted.

* To whom correspondence should be addressed: Department of Molecular Biosciences, 3004 Haworth Hall, University of Kansas, 1200 Sunnyside Ave., Lawrence, KS 66045-7534. Telephone: (785) 864-4727. Fax: (785) 864-5321. E-mail: xraymain@ku.edu.

[§] University of Kansas.

[||] Toyama Medical and Pharmaceutical University.

[⊥] University of Wisconsin Medical School.

[1] Abbreviations: SDH, serine dehydratase; PLP, pyridoxal 5′-phosphate; apo-SDH, PLP-free SDH; holo-SDH, PLP-bound SDH; OMS, *O*-methylserine; SDH−(OMS−PLP), OMS−PLP aldimine-bound SDH; SDH−(PLP−Ser), PLP−Ser aldimine-bound SDH.

10.1021/bi035324p CCC: $25.00
Published on Web 10/17/2003

enzyme has been shown to be involved in gluconeogenesis (*7*). The enzyme activity fluctuates depending on the available nutrients and in response to the levels of various hormones (*2*). The purified rat liver SDH is a dimer with an $M_r = 34\,200$ subunit (*8*−*11*). PLP binds to Lys41 to form a Schiff base, and the amino acid sequence (^{39}SXKIRG^{44}) is well-conserved among SDHs from rat (*12*), human (*13*), tomato (*14*), *Escherichia coli* (*15*, *16*), and yeast (*17*). These enzymes also have well-conserved sequences at ^{64}SAGN^{67} and a glycine-rich sequence at ^{168}GGGGL^{172} (*7*).

Nine crystal structures of PLP-dependent β-elimination enzymes have been determined. Those are *E. coli* threonine deaminase (*18*), *Salmonella typhimurium O*-acetylserine sulfhydrylase (*19*), *Synechocystis* L-cystine C-S lyase (*20*), *E. coli* selenocystine lyase (*21*), *Citrobacter freundii* tyrosine phenol-lyase (*22*), *S. typhimurium* tryptophan synthase (*23*), *Proteus vulgaris* tryptophanase (*24*), human cystathionine β-synthase (*25*), and *Arabidopsis* cystathionine β-lyase (*26*). Threonine deaminase, *O*-acetylserine sulfhydrylase, tryptophan synthase, and cystathionine β-synthase also catalyze the dehydration of serine. The *E. coli* threonine deaminase has the same function as rat liver SDH, but the bacterial enzyme is larger than the eukaryotic enzyme and is composed of the PLP-dependent catalytic domain and the regulatory domain (*18*). The crystal structure of *E. coli* threonine deaminase shows that the enzyme is a dimer of dimers and the catalytic and the regulatory domains are separated and have no interaction. The sequence of the catalytic domain is 27.7% identical with that of rat SDH. The β-subunit of *S. typhimurium* tryptophan synthase contains a PLP and catalyzes the synthesis of tryptophan from serine and indole (*23*). In the catalytic reaction, the substrate serine forms a PLP−Ser aldimine in the active site, and then the β-elimination reaction occurs to produce PLP−aminoacrylate. The catalytic domain structures of threonine deaminase and tryptophan synthase are quite similar and are expected to be similar to the structure of rat liver SDH.

Here we report crystal structures of apo-SDH and PLP−OMS aldimine-bound SDH. On the basis of these structures, a detailed catalytic mechanism of SDH is proposed, in which the resonance stabilization of PLP−Ser aldimine as observed in aminotransferases is not involved.

EXPERIMENTAL PROCEDURES

Purification and Crystallization Procedures. SDH used in this study is the recombinant rat enzyme produced in *E. coli* BL21 transformed with the pCW-SDH plasmid that contains the coding sequence of rat SDH cDNA (*27*). The enzyme was purified to homogeneity from *E. coli* extracts by ammonium sulfate precipitation, dialysis in 10 mM potassium phosphate buffer (pH 7.8) containing 5 mM cysteine, followed by gel filtration over Sephacryl S-200, and DEAE-cellulose chromatography as described previously (*27*). This procedure apparently removed the bound PLP and K^+ ion, and thus, we obtained the apoenzyme. The holoenzyme was prepared from the apoenzyme by incubation with 1 mM PLP, and the unbound PLP was removed by passing the compound through a Sephadex G-50 column.

The hanging-drop vapor-diffusion method was employed for crystallization of the enzyme. Crystals of the apoenzyme were grown in a solution containing 50 mM Tris-HCl buffer (pH 7.0), 1 mM dithiothreitol, 2% (w/v) PEG-3350, and 20% (v/v) ethylene glycol at a protein concentration of 10 mg/mL at 26 °C. Rice-shaped crystals suitable for X-ray diffraction studies (∼0.4 mm × 0.2 mm × 0.1 mm) were grown in a few days. Crystals of the holoenzyme were grown in a solution containing 50 mM HEPES buffer (pH 8.0), 10 mM DL-*O*-methylserine (OMS), 200 mM potassium acetate, 1 mM dithiothreitol, 14% (w/v) PEG-8000, and 2% 1,4-dioxane at a protein concentration of 20 mg/mL at 22 °C. Needle-shaped crystals suitable for X-ray diffraction studies (∼0.5 mm × 0.05 mm × 0.05 mm) were grown overnight.

Data Measurement. A crystal (0.4 mm × 0.2 mm × 0.1 mm) of the apoenzyme in a hanging drop was scooped up with a nylon loop and was dipped into a cryoprotectant solution containing 20% ethylene glycol, 50 mM Tris-HCl buffer (pH 7.0), and 5% (w/v) PEG-3350 for 30 s before the crystal was frozen in cold nitrogen gas (−180 °C) on a Rigaku RAXIS imaging plate X-ray diffractometer with a rotating anode X-ray generator as an X-ray source (Cu Kα radiation operated at 50 kV and 100 mA). The X-ray beam was focused to 0.3 mm by confocal optics (Osmic, Inc.). The diffraction data were measured up to 2.8 Å resolution at −180 °C. The data were processed with the program DENZO/SCALEPACK (*28*). The data statistics are given in Table 1. Data for the holoenzyme were obtained using a crystal (0.5 mm × 0.05 mm × 0.05 mm) with the same method used for the apoenzyme data measurement. The composition of the cryoprotectant for the holoenzyme was 20% (v/v) ethylene glycol, 50 mM HEPES buffer (pH 8.0), 200 mM potassium acetate, and 16% (w/v) PEG-8000.

The platinum derivative crystals were prepared by the soaking method; native crystals of the apoenzyme were incubated in an artificial mother liquor containing 50 mM Tris-HCl buffer (pH 7.0), 1 mM DTT, 5% (w/v) PEG-3350, 20% (v/v) ethylene glycol, and 1 mM K_2PtCl_4 for 10 min before they were frozen in liquid nitrogen. The diffraction data were measured up to 3.2 Å resolution at −180 °C and were processed with the same method used for the native data.

Determination of the Crystal Structure of Apo-SDH. The unit cell dimensions and the assigned space indicated that the asymmetric unit contains six subunits with a V_M of 2.80 Å^3. A difference Patterson map [$(F_{PH} - F_P)^2$ map] showed significant peaks corresponding to the Pt−Pt vectors. Twelve Pt positions in the asymmetric unit were determined by using the program CNS (*29*). The 12 Pt positions indicated that the six subunits are related by pseudo-32 symmetry. Initial protein phases were determined from the single isomorphous replacement (SIR) data in conjunction with solvent flattening using the programs in CNS. The electron density map was averaged by the pseudo-32 symmetry calculated from the Pt positions. The averaged electron density map showed three SDH dimers in an asymmetric unit. In each subunit, the main chains of 290 of 327 amino acid residues were traced continuously without any difficulty.

The crystal structure was refined by a standard refinement procedure in the CNS protocol with the noncrystallographic symmetry restraint. Six subunits were restrained to have similar conformations (i.e., rmsd < 0.08 Å). Refinement of isotropic temperature factors for individual atoms was carried out by the individual *B*-factor refinement procedure of CNS using bond and angle restraints. During the final refinement

Table 1: Crystallographic Statistics

	Diffraction Data		
	native	Pt derivative	PLP−OMS complex
resolution (Å)	35−2.8	35−3.2	35−2.6
unit cell	$a = 70.63$ Å, $b = 169.84$ Å, $c = 96.00$ Å, $\beta = 92.8°$	$a = 70.65$ Å, $b = 169.86$ Å, $c = 96.02$ Å, $\beta = 92.8°$	$a = 62.24$ Å, $b = 109.26$ Å $c = 98.94$ Å, $\beta = 91.7°$
space group	$P2_1$	$P2_1$	$P2_1$
total no. of observations	617721	376929	271545
no. of unique reflections	55569	37423	40796
completeness (%)	89.1	93.8	95.2
R_{merge}[a] (%)/outer shell[b]	7.0/13.9	9.3/15.0	7.8/12.4

	Phasing					
resolution range (Å)	34.5−5.98	∼4.75	∼4.15	∼3.77	∼3.50	∼3.20
phasing power[c] (acentric)	2.51	1.77	1.16	0.93	0.79	0.70
R_{Cullis}[d] (acentric)	0.53	0.66	0.78	0.83	0.87	0.91
R_{Cullis}[d] (anomalous)	0.69	0.83	0.84	0.92	0.94	1.19
figure of merit[e]	0.46	0.38	0.31	0.26	0.21	0.16

	Refinement	
	apo-SDH	SDH−(PLP−OMS)
no. of protein non-hydrogen atoms	13956	9668
no. of PLP−OMS molecules	−	96
no. of solvent molecules (H_2O)	105	119
resolution range (Å)	23.6−2.8	25.0−2.6
total no. of reflections used in R_{cryst}	47906	37708
total no. of reflections used in R_{free}	4806	3784
R_{cryst}[f] (outer shell)	0.22 (0.31)	0.23 (0.30)
R_{free} (outer shell)	0.25 (0.33)	0.26 (0.32)
rmsd for bond distances (Å)	0.009	0.009
rmsd for bond angles (deg)	1.4	1.4
rmsd for torsion angles (deg)	22.4	22.8
residues in most favored regions (%)	89.1	89.8
residues in additional allowed regions (%)	10.1	9.9
residues in generously allowed regions (%)	0.8	0.3

[a] $R_{merge} = \sum_h \sum_i |I_{hi} - \langle I_h \rangle| / \sum_h \sum_i |I_{hi}|$. [b] Outer shell, 2.8−2.9 Å resolution for apo-SDH and 2.7−2.6 Å resolution for SDH−(PLP−OMS). [c] Phasing power = mean F_H/(lack of closure). [d] R_{Cullis} = (lack of closure)/(isomorphous or anomalous difference). [e] Figure of merit = cosine of the likely error in the phase angles. [f] $R_{cryst} = \sum |F_o - F_c| / \sum |F_o|$.

stage, well-defined residual electron density peaks in difference maps were assigned to water molecules if peaks were able to bind to the protein molecules with hydrogen bonds. The final crystallographic *R*-factor was 0.222 for observed data (no σ cutoff) from 25 to 2.8 Å resolution. R_{free} for the randomly selected data (10%) equals 0.248.

Determination of the Crystal Structure of SDH−(PLP−OMS). The unit cell dimensions and space group indicated that an asymmetric unit contained four subunits with a V_M of 2.46 Å^3. The crystal structure was determined by a molecular replacement procedure using CNS (*29*). A subunit in the apo-SDH was used as the search model. The structure was refined with the simulated annealing procedure of CNS. The $2F_o - F_c$ maps calculated after refinement showed that several sections of the polypeptide had conformations different from those of the apoenzyme. The models of these amino acid sections were built in $2F_o - F_c$ maps. $F_o - F_c$ maps showed a large significant residual electron density peak in the region of the active site. Since SDH was crystallized in the presence of OMS (10 mM), PLP−OMS aldimine was fitted into the electron density peak. Other well-defined residual electron density peaks in $F_o - F_c$ maps were assigned to water molecules if peaks were able to bind the protein molecules with hydrogen bonds. One peak in each subunit that was significantly higher than those of water molecules was assigned to a potassium ion since the crystals were grown in a solution containing potassium ions (200 mM potassium acetate). The final model was refined by the simulated annealing procedure, and followed by the individual *B*-factor refinement procedure of CNS using bond and angle restraints. During the refinement, the four subunits related by a noncrystallographic symmetry were tightly restrained to have the same structure in an effort to increase the accuracy of coordinates. The final crystallographic *R*-factor was 0.231 for observed data (no σ cutoff) from 25 to 2.6 Å resolution. R_{free} for the randomly selected data (10%) equals 0.261. The coordinates have been deposited in the Protein Data Bank (entries 1PWE and 1PWH). Crystallographic parameters are listed in Table 1.

Determination of Molecular Weights in Solution by Dynamic Light Scattering. The molecular sizes and weights of the apo- and holoenzymes in solution were determined by using a dynamic light scattering apparatus (DynaPro, Protein Solution, Inc.). The apo- and holoenzymes (20 mg/mL) used for the above crystallization experiment were diluted in 50 mM Tris-HCl buffer (pH 7.0) or 50 mM potassium phosphate buffer (pH 7.0) to a protein concentration of 1 mg/mL. The dynamic light scatterings from the samples were measured at 20 and 30 °C, respectively. The data were analyzed with the associated program (Dynamics, version 5.25.44). The results are listed in Table 2.

RESULTS

Overall Crystal Structures. The crystallographic refinement parameters (Table 1), final $2F_o - F_c$ maps, and conformational analysis by PROCHECK (*30*) indicate that the crystal structures of apo-SDH and SDH−(PLP−OMS)

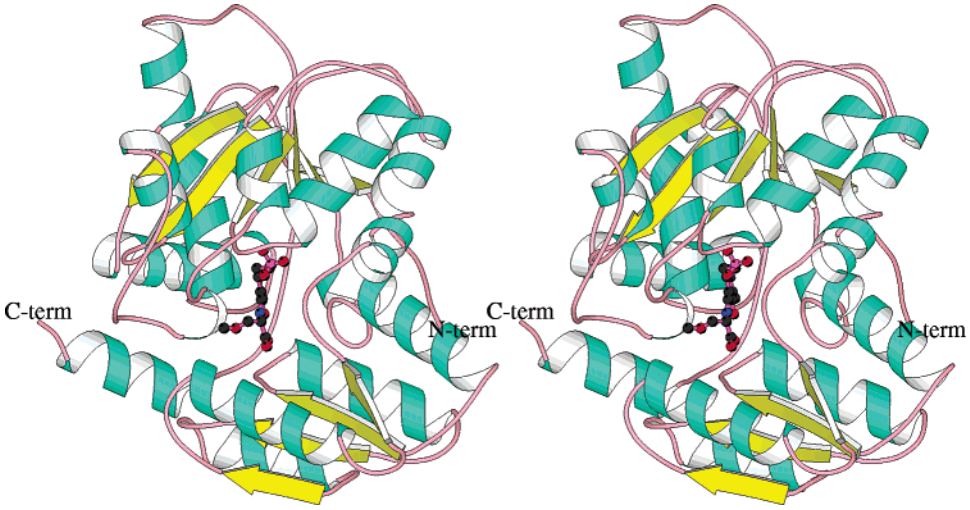

FIGURE 1: Ribbon drawing of SDH containing PLP−OMS aldimine viewed down the active site. The bound PLP−OMS aldimine is illustrated with a ball-and-stick diagram.

Table 2: Molecular Size and Weight in Solution Determined by Dynamic Light Scattering

	apoenzyme		holoenzyme	
condition (at 22 °C)	size (Å)	mass (kDa)	size (Å)	mass (kDa)
50 mM Tris-HCl buffer (pH 7) at 20 °C	37	72	33	56
50 mM Tris-HCl buffer (pH 7) at 30 °C	38	77	36	66
50 KP buffer (pH 7) at 20 °C	35	61	34	60
50 KP buffer (pH 7) at 30 °C	27	35	35	66

have been determined successfully. SDH is composed of two domains (the large domain being residues 1−35 and 137−327 and the small domain being residues 36−136). Each domain has an $\alpha\beta$-open structure (Figure 1). The active site is located between the domains. Although the overall structures of apo- and holoenzymes are quite similar to each other, they fold into different dimers (Figure 2).

Active Site Geometry. The active site of SDH−(PLP−OMS) contains PLP−OMS aldimine, indicating that OMS reacted with the bound PLP in the active site but the catalytic reaction was stopped after formation of the Schiff base (Figure 3). The bound PLP−OMS aldimine is mostly planar except for the phosphate group and the side chain of OMS (CH_2OCH_3) (Figure 4). The phosphate moiety of the bound PLP−OMS aldimine is surrounded by five amide groups of the conserved amino acid residues (^{168}GGGGL^{172}). The two oxygens (O_{1P} and O_{2P}) of the phosphate group form two hydrogen bonds with the amide groups of Gly168, Gly170, Gly171, and Leu172, and the third oxygen (O_{3P}) has one hydrogen bond with the amide group of Gly169, suggesting that the third oxygen can be protonated. Similarly, the carboxylate moiety is surrounded by the other conserved amino acid residues (^{64}SAGNA^{68}) and is involved in three hydrogen bonds with Ser64 O_G, Ala65 N, and Asn67 N (Figure 4). It is noteworthy that both negatively charged groups are in noncharged environments. Lys41, which forms a Schiff base linkage with the bound PLP, is located above the PLP plane, and its N_Z has a relatively short contact (2.7 Å) with the PLP $C_{4'}$. The N_Z is involved in hydrogen bonds with PLP O_3 and OMS O. Judging from the hydrogen bonding scheme, we find N_Z is neutral (i.e., $-NH_2$) and is the group that abstracts the α-hydrogen from C_A of the PLP−OMS aldimine. N_1 of PLP is involved in a hydrogen bond with the HS group of Cys303. A potassium ion is coordinated by six oxygen atoms (Gly168 O, Ala198 O, Leu223 O, Val225 O, Glu194 O_{E2}, and Ser200 O_G) near the active site. The major function of this ion is apparently to build the framework of the active site, but the ion is not involved in catalysis. Similar K^+ ions were found in the structures of β-elimination enzymes, tryptophan synthase (*23*) and tryptophanase (*24*). As discussed below, the structure of the apoenzyme does not contain the K^+ ion in the active site, and the polypeptide conformation from residue 193 to residue 234 is significantly different from that of the holoenzyme.

Model SDH−PLP and SDH−(PLP−Ser) Structures. On the basis of the SDH−(PLP−OMS) structure, the model structures before and after serine binding to the active site were built (Figure 5A,B). We assume that the bound PLP has the same interactions as seen in the SDH−(PLP−OMS) structure. For the SDH−PLP model, the OMS was removed, and the conformation of the side chain of Lys41 was changed so that N_Z can form a Schiff base linkage with $C_{4'}$ of bound PLP. Since the $N_Z-C_{4'}$ distance was still longer than the ideal C=N distance (1.34 Å), the PLP was tilted by 6° at the center of N_1 toward N_Z without breaking any hydrogen bonds (Figure 5A). For the SDH−(PLP−Ser) model, the OCH_3 group of OMS was replaced with an OH group, and the C_A-C_B bond was rotated by −133° so that O_G can form two hydrogen bonds with O of Ala222 and protonated O_{3P} of phosphate (Figure 5B).

Measurement of Molecular Sizes by Dynamic Light Scattering. Dynamic light scattering measurements indicate that the apo- and holoenzymes form a dimer in a 50 mM Tris-HCl buffer solution (pH 7.0) at 20 and 30 °C. However, in a 50 mM potassium phosphate buffer solution (pH 7.0), the apoenzyme becomes a monomer at 30 °C, while the holoenzyme is still dimers. The results indicate that the apo- and holoenzymes form different dimers and the apo dimer is unstable in solution containing a high concentration of K^+ ion. This is consistent with the crystal structures described above.

DISCUSSION

Apo- and Holoenzymes Form Different Dimers. In the apoenzyme structure, the two subunits form a dimer related

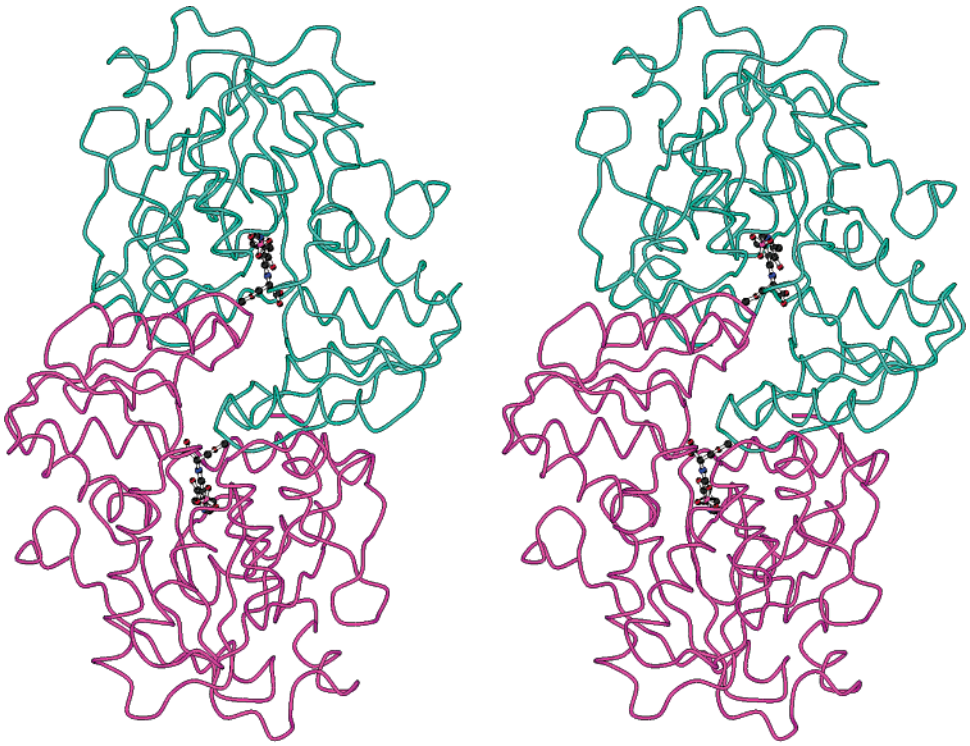

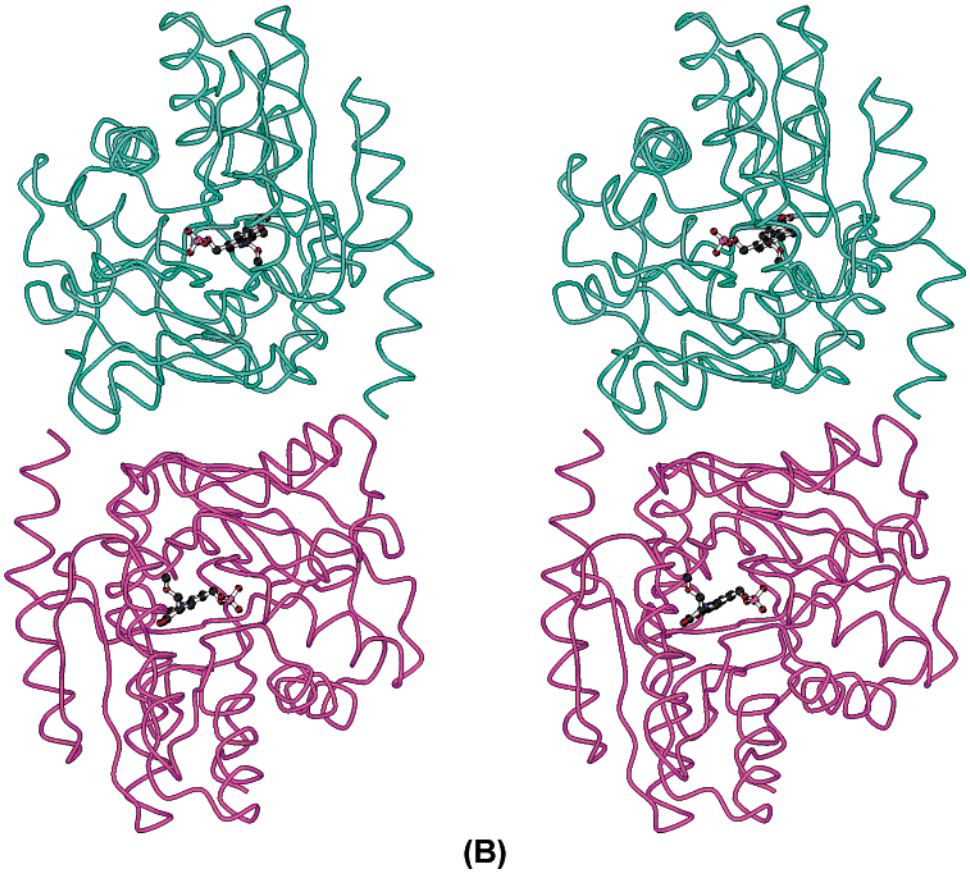

FIGURE 2: Two dimer structures seen in apo- and holo-SDH. The dimers are viewed down the noncrystallographic 2-fold axis: (A) apo-SDH and (B) SDH−(PLP−OMS). Two subunits are colored aquamarine and magenta. The active sites are indicated by incorporating a model of PLP−OMS aldimine.

by noncrystallographic 2-fold symmetry (Figure 2A). In the dimer structure, the small domain is rotated by 7.2° to open the active site cleft, and the small domain of the partner subunit enters the opened cleft. Since the small domain of the partner subunit blocks the entrance to the active site, the enzyme is an inactive form. Similar dimerization is seen in the structure of PLP-dependent alanine racemase (*31*). In the SDH−(PLP−OMS) structure, two subunits form a dimer by

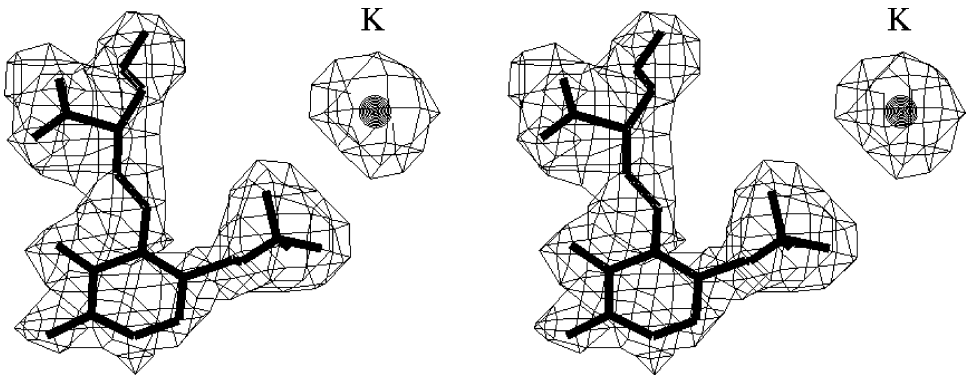

FIGURE 3: $2F_o - F_c$ maps showing the electron density peaks of the PLP−OMS aldimine and K^+ ion in the active site. The contour is drawn at the 1.2σ level.

Table 3: Comparison between the Tertiary Structures of Rat SDH and β-Elimination Enzymes

(1) Number of C_A Atoms which Can Be Superimposed on the SDH Structure

enzyme	PDB code	no. of residues	no. of C_A atoms superimposed (%)	rmsd (Å)	identical residues (%)
SDH	1PWH	327	327 (100%)	0.00	100
threonine deaminase	1TDJ	494	286 (87%)	1.98	24
tryptophan synthase (β-subunit)	1QOP	391	278 (85%)	2.04	20
O-acetylserine sulfhydrylase	1OAS	315	274 (84%)	2.21	24
cystathionine β-synthase	1JBQ	435	142 (43%)	2.21	17
tyrosine phenol-lyase	2TPL	456	70 (21%)	2.54	8
L-cystine C-S lyase	1ELU	393	67 (20%)	2.45	10
selenocystine lyase	1JF9	406	64 (19%)	2.70	7
tryptophanase	1AX4	466	45 (13%)	2.56	17
cystathionine β-lyase	1IBJ	464	39 (11%)	2.75	12

(2) Hydrogen Bond Partners of N_1 and the Phosphate Group of PLP

enzyme	hydrogen bond partner of N_1	hydrogen bond partners of the phosphate group
SDH	C303 S_G	G168 N, G169 N, G170 N, G171 N, L172 N
threonine deaminase	S315 O_G	G188 N, G189 N, G190 N, G191 N, L192 N
tryptophan synthase (β-subunit)	S377B O_G	G232B N, G233B N, G234B N, S235B N, N236B N, T190B O_{G1}, S235B O_G, N236B N_{D2}
O-acetylserine sulfhydrylase	S272A O_G	G176 N, T177 N, G178 N, T180 N, 177 O_{G1}, T180 O_{G1}
cystathionine β-synthase	S349 O_G	G256 N, T257 N, T257 O_{G1}, G258 N, T260 N, T260 O_{G1}, H_2O
tyrosine phenol-lyase	D214B O_{D2}	G99B N, R110B N_E, R110B N_{H2}, S254B O_G
L-cystine C-S lyase	D197 O_{D1}	V88 N, T89 N, T89 O_{G1}, H22 N_{E2}, W251B N_{E1}, T276B O_{G1}
selenocystine lyase	D200 O_{D2}	T95 N, T278* N, T95 O_{G1}, S223 O_G, H255 N_{E2}, T278* O_{G1}
tryptophanase	D223 O_{D2}	Q99 N_{E2}, G100 N, R101 N, R101 N_E, R101 N_{H2}, S263 O_G, $2H_2O$
cystathionine β-lyase	D253 O_{D2}	G157 N, M158 N, S275 O_G, T277 O_{G1}, Y127* O_H, R129* N_E, R129* N_{H2}

making contacts at the back of the two clefts so that the entrance of the active site is open, and thus, the enzyme is an active form. Similar dimerization is seen in the structure of *E. coli* threonine deaminase which is a tetramer (dimer of dimers) related by a crystallographic 222 symmetry (*18*).

Compared with the subunits of the holoenzyme dimer, the subunits in the apoenzyme dimer interact extensively. The major difference between the apo- and holoenzyme is seen in the polypeptide conformation of residues 197−228, which do not interact with the bound PLP. As shown in Figure 6, the two polypeptides fold completely differently. When the holoenzyme loses the cofactor PLP and K^+ ion, residues 197−228 undergo a large conformational change to evacuate the site that residues 105−124 of the partner subunit will occupy. The subunits of the holoenzyme cannot form a dimer similar to that seen in the apoenzyme, but the subunits of the apoenzyme can form a dimer similar to that seen in the holoenzyme, suggesting that the apo-type dimer is more stable than the holo-type dimer. The bound PLP and K^+ ion readily dissociate from the enzyme by simple dialysis in the presence of cysteine (*32*), suggesting the presence of the apo-type dimers in cells.

The mammalian liver enzymes are involved in gluconeogenesis, whereas the microorganism enzymes are involved mainly in isoleucine biosynthesis. The *E. coli* enzyme (threonine deaminase) is composed of the catalytic and regulatory domains, and is regulated by feedback regulation (i.e., inhibited by the end product isoleucine). The regulation scheme of the mammalian liver enzyme is unknown. As described above, rat liver SDH forms two different dimers, and the bound PLP readily dissociates from SDH in the presence of free cysteine. When the free cysteine level is

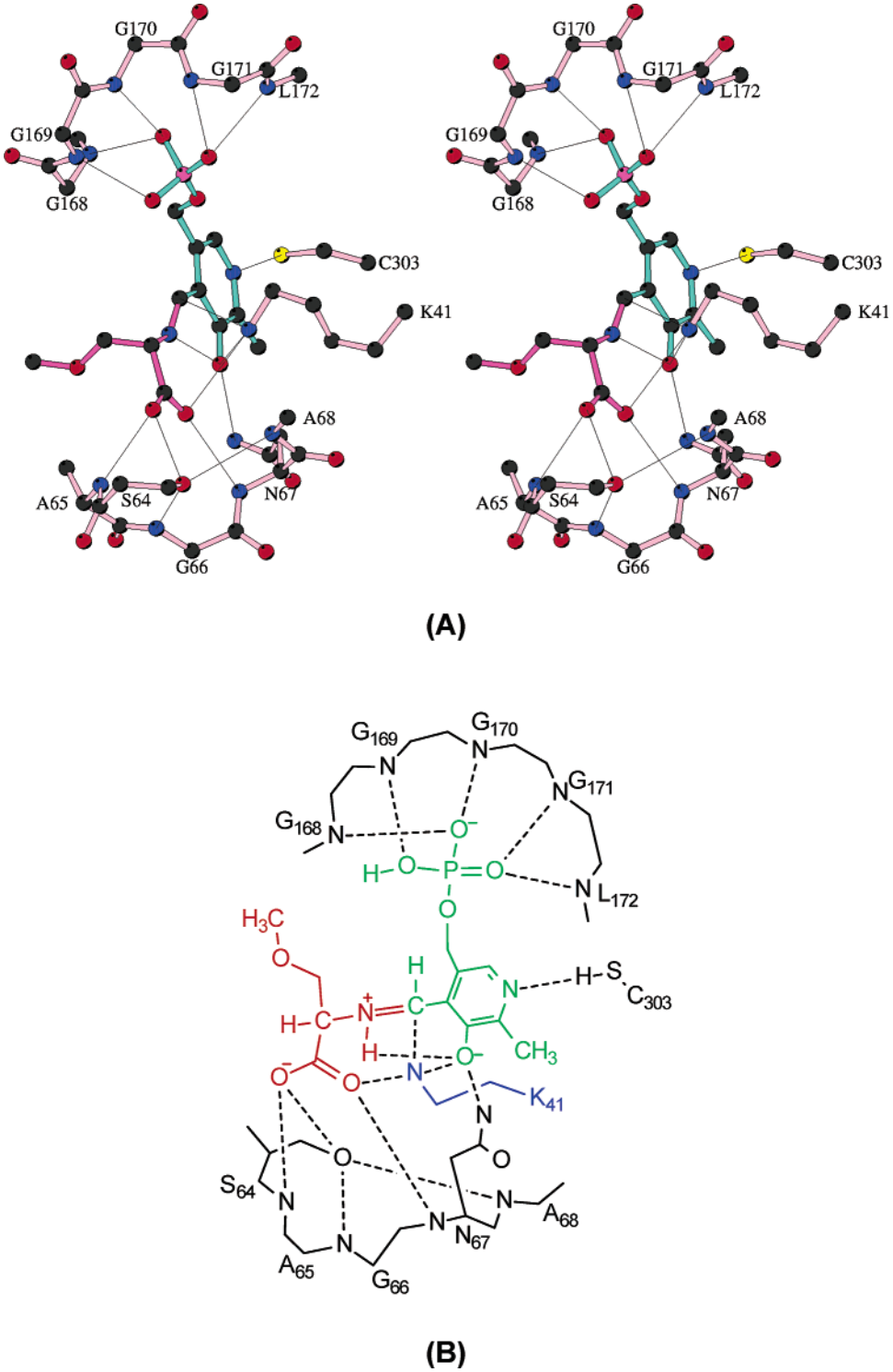

FIGURE 4: Possible interactions between SDH and PLP−OMS aldimine. (A) PLP−OMS aldimine in the active site. Possible hydrogen bonds between PLP−OMS aldimine and SDH are represented by thin lines. (B) Schematic diagram showing the interaction of PLP−OMS aldimine in the active site. Dashed lines represent the possible hydrogen bonds.

relatively high in the cell, the rat liver SDH loses the bound PLP and K^+ ion and shifts the conformational equilibrium to the apo-type conformation. The apoenzymes are stabilized by forming the new type of dimer. This study suggests that the level of free cysteine would regulate the liver enzyme.

β-Elimination Enzymes Are Divided into Two Groups. Crystal structures of nine PLP-dependent β-elimination enzymes are known. These are *E. coli* threonine deaminase (*18*), *O*-acetylserine sulfhydrylase (*19*), rat SDH (this study), L-cystine C-S lyase (*20*), selenocystine lyase (*21*), tyrosine phenol-lyase (*22*), the β-subunit of tryptophan synthase (*23*), *P. vulgaris* tryptophanase (*24*), human cystathionine β-synthase (*25*), and *Arabidopsis* cystathionine β-lyase (*26*). The overall structures of the PLP-binding domains of these enzymes are quite similar to each other. However, as shown in Table 3, these enzymes are clearly divided into two groups when the structures are compared to the SDH structure.

For the following discussion, it is important to determine whether N_1 of the bound PLP is protonated. Since S_G of Cys303 is located near the C_4-N_1 vector of the bound PLP

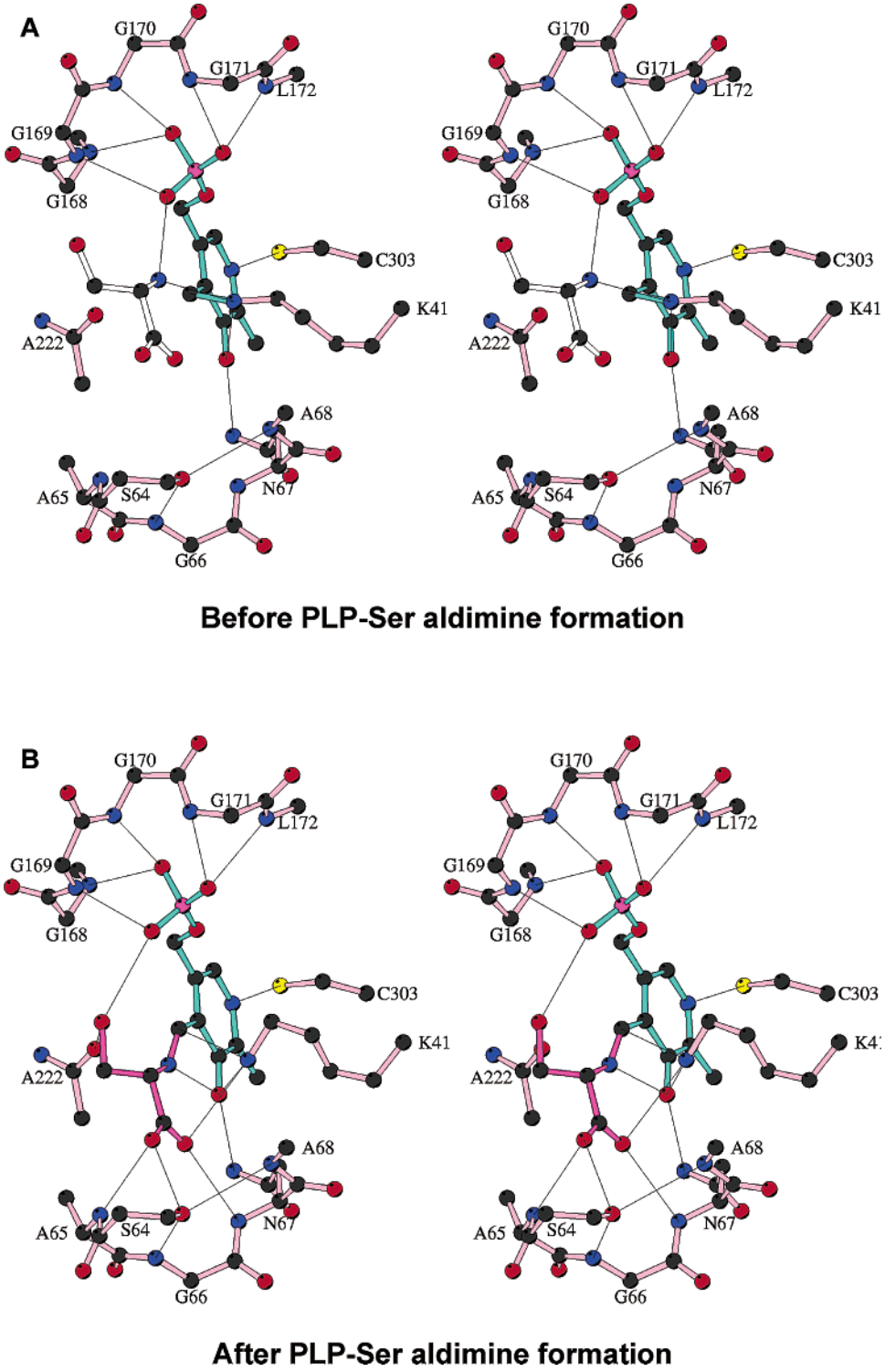

FIGURE 5: Model structures before and after formation of PLP−OMS aldimine.

with a $S_G \cdots N_1$ distance of 2.96 Å and a $C_B-S_G \cdots N_1$ angle of 89°, S_G forms a hydrogen bond with N_1. Also, S_G of Cys303 has a short contact (3.57 Å) with S_G of Cys270 which forms a hydrogen bond with the amide group of Gly304 (S···N distance of 3.41 Å). Under neutral conditions, S_G of Cys303 forms a $S-H \cdots N$ hydrogen bond with N_1. Thus, N_1 of the bound PLP is not protonated. However, since the hydrogen of the sulfhydryl group of cysteine can be dissociated, we cannot exclude an $^{-}S \cdots H-N^{+}$ hydrogen bond in a basic environment. As will be described below, a serine residue is located at the same site of Cys303 in the structures of threonine deaminase (*18*), tryptophan synthase (*23*), *O*-acetylserine sulfhydrylase (*19*), and cystathionine *β*-synthase (*25*). The $C_A-C_B-O_G$ moieties of the serine residues are located at the same place as the $C_A-C_B-S_G$ moiety of Cys303, and thus, the O_G groups participate in a hydrogen bond with N_1 of the bound PLP. Since the hydrogen of the hydroxyl group of serine residue cannot be dissociated, it is possible to determine whether the hydrogen bond is of the Ser OH···N PLP or Ser $HO \cdots HN^{+}$ PLP form by examining the hydrogen bonding scheme around the serine residue. A careful examination of the hydrogen bond

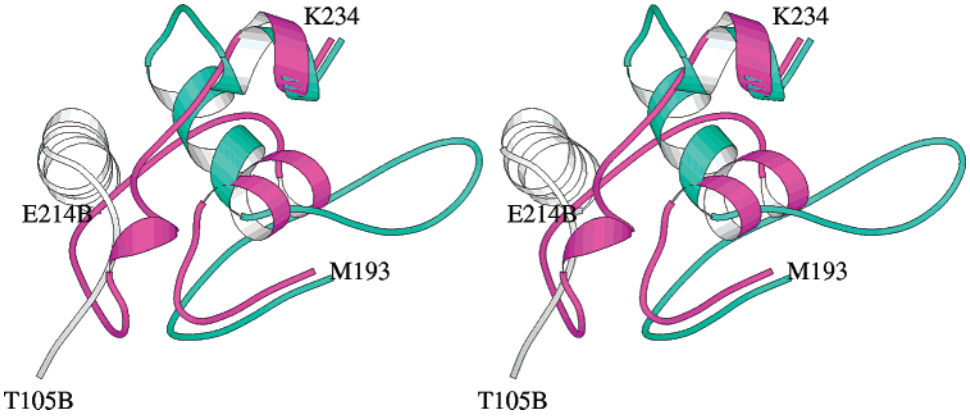

FIGURE 6: Superimposed view of amino acid residues 193−234 showing a large conformational difference between the apoenzyme (aquamarine) and holoenzyme (magenta). Amino acid residues 105−124 of the partner subunit of the apoenzyme are shown in white.

networks around the serine residues in the structures of threonine deaminase, tryptophan synthase, *O*-acetylserine sulfhydrylase, and cystathionine β-synthase indicates that the hydrogen bond between the serine and the bound PLP is an OH···N bond and N_1 is not protonated. Since serine and cysteine are structurally similar and the catalytic functions of SDH, threonine deaminase, tryptophan synthase, *O*-acetylserine sulfhydrylase, and cystathionine β-synthase are the same (i.e., these enzymes catalyze the cleavage of the C_B-O_G bond of serine), it is reasonable to conclude that N_1 of the bound PLP in the SDH structure is not protonated.

Threonine deaminase, tryptophan synthase, *O*-acetylserine sulfhydrylase, cystathionine β-synthase, and SDH belong to the first group for the following reasons. (1) Their structures are very similar because more than 84% of the C_A atoms of SDH superimpose on their C_A atoms. (2) The N_1 atoms of PLP are nonprotonated because the hydrogen bond partner of the N_1 atoms is a neutral amino acid residue. (3) The phosphate groups are in the less polarized form (HPO_4^-) because they are surrounded mainly by backbone amide groups and not charged amino acids. (4) All these enzymes catalyze the cleavage of the C_B-O bond of Ser/Thr.

L-Cystine C-S lyase, selenocystine lyase, tyrosine phenol-lyase, tryptophanase, and cystathionine β-lyase belong to the second group for the following reasons. (1) Their similarities to SDH are relatively poor because less than 21% of the C_A atoms of SDH superimpose on their C_A atoms. (2) The N_1 atoms of PLP are protonated because the hydrogen bond partner of the N_1 atoms is a negatively charged amino acid residue. (3) The phosphate groups are in the more polarized form (PO_4^{2-}) because the environment surrounding the phosphate groups contains positively charged amino acid residues and fewer backbone amide groups. (4) These enzymes catalyze cleavage of the C_B-S or C_B-C bond.

It has been believed that N_1 of the PLP pyridine is protonated by an acidic amino acid residue, and thus, the pyridine ring of PLP can form the quinone-like resonance structure. The α-hydrogen of the PLP−amino acid aldimine is readily abstracted by a basic residue (Schiff base Lys) because the resulting carbanion can form the resonance-stabilized structure, whereas N_1 of the PLP pyridine is not protonated in the structures of SDH, threonine deaminase, tryptophan synthase, *O*-acetylserine sulfhydrylase, and cystathionine β-synthase. The α-hydrogen abstraction is not as easy as in the cases with protonated pyridine because the resulting carbanion cannot form the resonance-stabilized structure. Therefore, an additional mechanism for stimulating α-hydrogen abstraction is required. This mechanism is most likely cleavage of the C_B-O bond by a strong acid. As described above, it is reasonably assumed that SDH, threonine deaminase, tryptophan synthase, *O*-acetylserine sulfhydrylase, and cystathionine β-synthase use the same catalytic mechanism to cleave the C_B-O bond and have the same essential amino acid residue (a strong acid) for cleavage of the C_B-O bond. Such an amino acid residue should be located near serine of the PLP−Ser aldimine in the structures of SDH, threonine deaminase, tryptophan synthase, and *O*-acetylserine sulfhydrylase. Since the published structures of threonine deaminase, *O*-acetylserine sulfhydrylase, and cystathionine β-synthase do not contain the PLP−Ser aldimine, these structures are not used for this analysis. Two groups have determined the crystal structures of tryptophan synthase containing a PLP−Ser aldimine. Rhee *et al.* mutated the Schiff base lysine (Lys87) to threonine and trapped a PLP−Ser aldimine in the active site of the mutated enzyme (*33*). O_G of the PLP−Ser aldimine is involved in two hydrogen bonds ($O_GH\cdots O_{D1}$ Asp305 and Ala112 $NH\cdots O_G$). The β-elimination reaction could not occur in this geometry because the amide group cannot be a sufficiently strong acid to donate a proton to the leaving O_G. Furthermore, Asp305 is not conserved in the structure of SDH (the corresponding amino acid is Gly224). Therefore, the structure of K87T mutant tryptophan synthase does not suggest any essential amino acid residue for cleavage of the C_B-O bond. The second group, Schneider *et al.*, trapped a PLP−aminoacrylate aldimine in the active site by using an inhibitor, 5-fluoroindole propanol phosphate, under steady state conditions (*34*). The amino acid residues in the active site are the same as those of the K87T mutant enzyme except for Lys87 and Asp305. The side chain of Asp305 is oriented in the opposite direction and away from the serine. This structure indicates again that Asp305 is not the essential amino acid residue. In conclusion, there is no amino acid residue that can act as a strong acid to donate a proton to the leaving O_G of serine. As will be explained below, we propose that the phosphate group of PLP surrounded by backbone amide groups acts as a strong acid to donate a proton to O_G of serine. The other possible strong acid would be the Schiff base lysine if a relatively large conformational change were allowed.

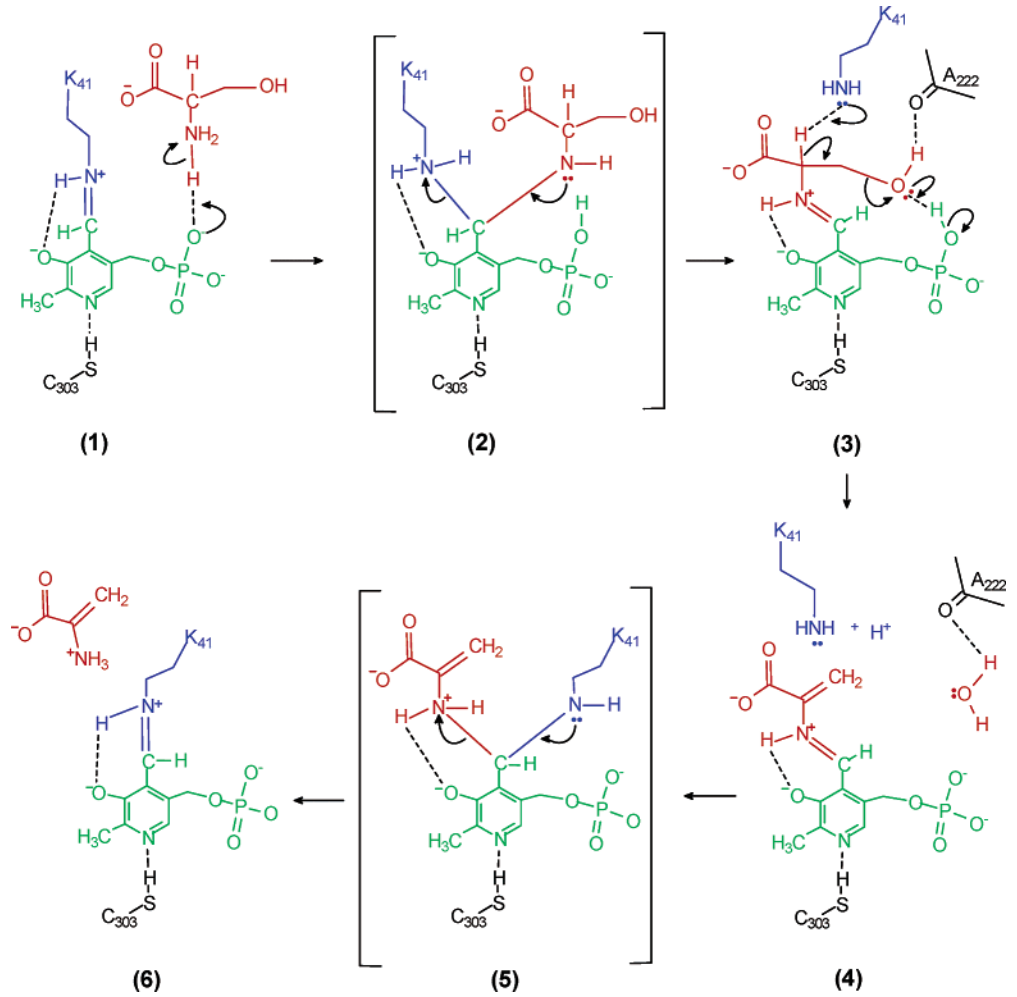

FIGURE 7: Proposed catalytic mechanism of SDH. Arrows indicate movement of electrons. Possible hydrogen bonds are represented by dashed lines. (1) A serine molecule enters the active site. The amino group forms a hydrogen bond with the phosphate. The proton in the hydrogen bond moves to the phosphate. The amino group becomes a nucleophile. (2) The amino group attacks the enzyme−PLP Schiff base carbon atom ($C_{4'}$) to produce the ternary complex intermediate (geminal diamine intermediate). (3) Lys41 is released from the PLP, and PLP−Ser aldimine is produced. The phosphate group acts as a general acid to donate the proton to O_G of the serine molecule. Abstraction of the α-hydrogen from C_A by Lys41 occurs in a concerted fashion. (4) A water molecule is released, and the PLP−aminoacrylate intermediate is produced. (5) Lys41 approaches $C_{4'}$, and the ternary complex intermediate is formed. (6) Aminoacrylate is released, and the enzyme−PLP Schiff base is re-formed.

It is noted that Scarselli *et al*. (*35*) have proposed a model structure of rat SDH based on the crystal structure of *E. coli* threonine deaminase. Although the phosphate pocket geometry agrees with this crystal structure, the other important amino acid residues do not correspond with those found in this crystal structure, suggesting a limitation of the molecular modeling.

Proposed Catalytic Mechanism of SDH. On the basis of the crystal structure of SDH−(PLP−OMS) along with the characteristic amino acid sequence of SDH, the model structures of SDH−PLP and SDH−(PLP−Ser), and the crystal structures of tryptophan synthase discussed above, a possible SDH catalytic mechanism is described below and illustrated in Figure 7.

(1) In the holoenzyme, Lys41 is located above the PLP plane, and its N_Z is connected to $C_{4'}$ of PLP by a Schiff base linkage. The phosphate group of PLP is in a pocket composed of the conserved G-rich section (^{168}GGGGL^{172}). A serine molecule enters the active site with its positively charged amino group pointing to the negatively charged phosphate group of PLP, and approaches the PLP along the plane of PLP, which is an ideal geometry for formation of the PLP−Ser aldimine.

(2) Initially, the amino group of serine forms a hydrogen bond with the phosphate, and the proton in the hydrogen bond moves to the phosphate. The phosphate is protonated, and the amino group becomes a nucleophile. The nucleophilic amino group attacks the enzyme−PLP Schiff base carbon atom ($C_{4'}$) to form a PLP−Ser aldimine and to release the neutral Lys41 from the bound PLP.

(3) The carboxylate group of serine is bound to the conserved section (^{64}SAGNA^{68}) of the protein, while the hydroxyl group (O_GH) participates in two hydrogen bonds ($O_GH\cdots$O Ala222 and PLP $O_{3P}H\cdots O_G$).

(4) Since N_1 of PLP is not protonated, the pyridine ring cannot take a quinone-like structure. Therefore, abstraction of the α-hydrogen from C_A of serine by Lys41 would not occur. However, since the $O_{3P}H$ group can act as a general acid to donate the proton to O_G of serine, abstraction of the α-hydrogen from C_A by Lys41 occurs in a concerted fashion. This catalytic reaction produces water and a PLP−aminoacrylate intermediate.

(5) Lys41 approaches $C_{4'}$ and forms a Schiff base linkage to the PLP, and aminoacrylate is released.

(6) The released aminoacrylate is deaminated to pyruvate by nonenzymatic hydrolysis.

Differences between SDH and Aminotransferase. PLP is involved in a variety of enzyme reactions such as transamination, decarboxylation, isomerization, and elimination (*36*). These PLP-dependent enzymes have similar overall structures. When the environments around the PLP−amino acid aldimine in the SDH and aminotransferase (*37*) structures are compared, there are three major differences.

(1) The ring N_1 in SDH is involved in a hydrogen bond with Cys and is neutral (N···H−S); on the other hand, in aminotransferases, the hydrogen bond partner of N_1 is Asp/Glu, and thus, N_1 is protonated ($^+$N−H···O$^-$).

(2) The phosphate group in SDH is in a neutral environment and thus is less polarized (i.e., HPO_3^-), whereas in aminotransferases, the phosphate group interacts with positively charged amino acid residues (Arg/Lys) and thus is polarized (i.e., PO_3^{2-}).

(3) The carboxylate group in SDH is in a neutral environment and thus is less polarized, whereas the carboxylate group in aminotransferases interacts with positively charged amino acid residues (Arg/Lys) and thus is polarized.

These differences apparently determine β-elimination for SDH and the deamination for aminotransferases. In the aminotransferases, the protonated pyridine ring can assume a quinone-like structure and participate in the resonance stabilization of the carbanion on C_A. N_1 to the carbonyl oxygen of the amino acid can participate in resonance stabilization because the aldimine is mainly planar and the carboxylate is polarized by surrounding positively charged amino acid residues (Arg/Lys). Eventually, the carbanion reacts with a water molecule, and the PLP−amino acid carbanion becomes pyridoxamine 5′-phosphate and a keto acid to complete the deaminase reaction.

For SDH, since N_1 in SDH is not protonated, the pyridine ring cannot assume a quinone-like structure. Furthermore, the carboxylate group is less polarized. For these reasons, the carbanion on C_A is not stabilized by the resonance structure observed in the aminotransferases. Therefore, it is more difficult to abstract the α-hydrogen from the amino acid in the aldimine. As we proposed above, the phosphate group surrounded by the characteristic amino acid sequence (^{168}GGGGL^{172}) becomes a strong general acid and donates a proton to the leaving O_G of serine. Consequently, the α-hydrogen is readily abstracted by Lys41, and the PLP−Ser aldimine becomes the PLP−aminoacrylate aldimine.

ACKNOWLEDGMENT

We thank Professor Richard H. Himes and Mr. Ken Takusagawa for a critical reading of the manuscript and very valuable comments.

REFERENCES

1. Holzer, H., Cennamo, C., and Boll, M. (1964) Product activation of yeast threonine dehydratase by ammonia, *Biochem. Biophys. Res. Commun. 14*, 487−492.
2. Snell, K. (1984) Enzymes of serine metabolism in normal, developing and neoplastic rat tissues, *Adv. Enzyme Regul. 22*, 325−400.
3. Reiber, H. (1974) Proceedings: Alpha, beta-elimination of serine: mechanism and catalysis of a model reaction and the consequences for the active centre of serine dehydratases, *Hoppe Seyler's Z. Physiol. Chem. 355*, 1240.
4. Alexander, F. W., Sandmeier, E., Mehta, P. K., and Christen, P. (1994) Evolutionary relationships among pyridoxal-5′-phosphate-dependent enzymes. Regio-specific α, β, and γ families, *Eur. J. Biochem. 219*, 953−960.
5. Umbarger, H. E. (1992) The origin of a useful concept: feedback inhibition, *Protein Sci. 1*, 1392−1395.
6. Changeux, J.-P. (1993) Allosteric proteins: from regulatory enzymes to receptors−personal recollections, *BioEssays 15*, 625−634.
7. Ogawa, H. (2000) Structure and function relationships of serine dehydratases from various sources, *Trends Comp. Biochem. Physiol. 6*, 1−19.
8. Ogawa, H., Miller, D. A., Dunn, T., Su, Y., Burcham, J. M., Peraino, C., Fujioka, M., Babcock, K., and Pitot, H. C. (1988) Isolation and nucleotide sequence of the cDNA for rat liver serine dehydratase mRNA and structures of the 5′ and 3′ flanking regions of the serine dehydratase gene, *Proc. Natl. Acad. Sci. U.S.A. 85*, 5809−5813.
9. Ogawa, H., Fujioka, M., Date, T., Mueckler, M., Su, Y., and Pitot, H. C. (1990) Rat serine dehydratase gene codes for two species of messenger RNA of which only one is translated into serine dehydratase, *J. Biol. Chem. 265*, 14407−14413.
10. Leoncini, R., Henschen, A., Krieglstein, K., Calvete, J., Pagani, R., and Marinello, E. (1990) Primary Structure of Rat Liver L-Threonine Deaminase, *Ital. J. Biochem. 39*, 228−234.
11. Ogawa, H., Gomi, T., Takusagawa, F., Masuda, T., Goto, T., Kan, T., and Huh, N. H. (2002) Evidence for a dimeric structure of rat liver serine dehydratase, *Int. J. Biochem. Cell Biol. 34*, 533−543.
12. Ogawa, H., Konishi, K., and Fujioka, M. (1989) The peptide sequences near the bound pyridoxal phosphate are conserved in serine dehydratase from rat liver and threonine dehydratases from yeast and *Escherichia coli*, *Biochim. Biophys. Acta 996*, 139−141.
13. Ogawa, H., Gomi, T., Konishi, K., Date, T., Nakashima, H., Nose, K., Matsuda, Y., Peraino, C., Pitot, H. C., and Fujioka, M. (1989) Human liver serine dehydratase: cDNA cloning and sequence homology with hydroxyamino acid dehydratases from other sources, *J. Biol. Chem. 264*, 15818−15823.
14. Samach, A., Hareven, D., Gutfinger, T., Ken-Dror, S., and Lifschitz, E. (1991) Biosynthetic threonine deaminase gene of tomato: Isolation, structure, and upregulation in floral organs, *Proc. Natl. Acad. Sci. U.S.A. 88*, 2678−2682.
15. Datta, P., Goss, T. J., Omnaas, J. R., and Patil, R. V. (1987) Covalent structure of biodegradative threonine dehydratase of *Escherichia coli*: Homology with other dehydratases, *Proc. Natl. Acad. Sci. U.S.A. 84* 393−397.
16. Eisenstein, E., Yu, H. D., Fisher, K. E., Iacuzio, D. A., Ducote, K. R., and Schwarz, F. P. (1995) An expanded two-state model accounts for homotropic cooperativity in biosynthetic threonine deaminase from *Escherichia coli*, *Biochemistry 34*, 9403−9412.
17. Bornaes, C., Petersen, J. G. L., and Holmberg, S. (1992) Serine and threonine catabolism in *Saccharomyces cerevisiae*: The CHA1 polypeptide is homologous with other serine and threonine dehydratases, *Genetics 131*, 531−539.
18. Gallagher, D. T., Gilliland, G. L., Xiao, G., Zondlo, J., Fisher, K. E., Chinchilla, D., and Eisenstein, E. (1998) Structure and control of pyridoxal phosphate dependent allosteric threonine deaminase, *Structure 15*, 465−475.
19. Burkhard, P., Rao, G. S., Hohenester, E., Schnackerz, K. D., Cook, P. F., and Jansonius, J. N. (1998) Three-dimensional structure of *O*-acetylserine sulfhydrylase from *Salmonella typhimurium*, *J. Mol. Biol. 283*, 121−133.
20. Clausen, T., Kaiser, J. T., Steegborn, C., Huber, R., and Kessler, D. (2000) Crystal structure of the cystine C−S lyase from *Synechocystis*: Stabilization of cysteine persulfide for FeS cluster biosynthesis, *Proc. Natl. Acad. Sci. U.S.A. 97*, 3856−3861.
21. Lima, C. D. (2002) Analysis of the *E. coli* NifS CsdB protein at 2.0 Å reveals the structural basis for perselenide and persulfide intermediate formation, *J. Mol. Biol. 315*, 1199−1208.
22. Sundararaju, B., Antson, A. A., Phillips, R. S., Demidkina, T. V., Barbolina, M. V., Gollnick, P., Dodson, G. G., and Wilson, K. S. (1997) The crystal structure of *Citrobacter freundii* tyrosine phenol-lyase complexed with 3-(4′-hydroxyphenyl)propionic acid, together with site-directed mutagenesis and kinetic analysis, demonstrates that arginine 381 is required for substrate specificity, *Biochemistry 36*, 6502−6510.

23. Hyde, C. C., Ahmed, S. A., Padlan, E. A., Miles, E. W., and Davies, D. R. (1988) Three-dimensional structure of the tryptophan synthase $\alpha_2\beta_2$ multienzyme complex from *Salmonella typhimurium*, *J. Biol. Chem. 263*, 17857−17871.
24. Isupov, M. N., Antson, A. A., Dodson, E. J., Dodson, G. G., Dementieva, I. S., Zakomirdina, L. N., Wilson, K. S., Dauter, Z., Lebedev, A. A., and Harutyunyan, E. H. (1998) Crystal structure of tryptophanase, *J. Mol. Biol. 276*, 603−623.
25. Meier, M., Janosik, M., Kery, V., Kraus, J. P., and Burkhard, P. (2001) Structure of human cystathionine β-synthase: A unique pyridoxal 5′-phosphate-dependent heme protein, *EMBO J. 20*, 3910−3916.
26. Breitinger, U., Clausen, T., Ehlert, S., Huber, R., Laber, B., Schmidt, F., Pohl, E., and Messerschmidt, A. (2001) The three-dimensional structure of cystathionine β-lyase from *Arabidopsis* and its substrate specificity, *Plant Physiol. 126*, 631−642.
27. Ogawa, H., Takusagawa, F., Wakaki, K., Kishi, H., Eskandarian, M. R., Kobayashi, M., Date, T., Huh, N.-H., and Pitot, H. C. (1999) Rat liver serine dehydratase. Bacterial expression and two folding domains as revealed by limited proteolysis, *J. Biol. Chem. 274*, 12855−12860.
28. Otwinowski, Z., and Minor, W. (1997) Processing of X-ray diffraction data collected in oscillation mode, *Methods Enzymol. 276*, 307−326.
29. Brünger, A. T., Adams, P. D., Clore, G. M., DeLano, W. L., Gros, P., Grosse-Kunstleve, R. W., Jiang, J. S., Kuszewski, J., Nilges, M., Pannu, N. S., Read, R. J., Rice, L. M., Simonson, T., and Warren, G. L. (1998) Crystallography and NMR system: A new software suite for macromolecular structure determination, *Acta Crystallogr. D54*, 905−921.
30. Laskowski, R. A., MacArthur, M. W., Moss, D. S., and Thornton, J. M. (1993) PROCHECK: A program to check the stereochemical quality of protein structures, *J. Appl. Crystallogr. 26*, 283−291.
31. Shaw, J. P., Petsko, G. A., and Ringe, D. (1997) Determination of the structure of alanine racemase from *Bacillus stearothermophilus* at 1.9 Å resolution, *Biochemistry 36*, 1329−1342.
32. Nakagawa, H., and Kimura, H. (1969) The properties of crystalline serine dehydratase of rat liver, *J. Biochem. 66*, 669−683.
33. Rhee, S., Parris, K. D., Hyde, C. C., Ahmed, S. A., Miles, E. W., and Davies, D. R. (1997) Crystal structures of a mutant (βK87T) tryptophan synthase $\alpha2\beta2$ complex with ligands bound to the active sites of the α- and β-subunits reveal ligand-induced conformational changes, *Biochemistry 36*, 7664−7680.
34. Schneider, T. R., Gerhardt, E., Lee, M., Liang, P. H., Anderson, K. S., and Schlichting, I. (1998) Loop closure and intersubunit communication in tryptophan synthase, *Biochemistry 37*, 5394−5406.
35. Scarselli, M., Padula, M. G., Bernini, A., Spiga, O., Ciutti, A., Leoncini, R., Vannoni, D., Marinello, E., and Niccolai, N. (2003) Structure and function correlations between the rat liver threonine deaminase and aminotransferases, *Biochim. Biophys. Acta 1645*, 40−48.
36. John, R. A. (1995) Pyridoxal phosphate-dependent enzymes, *Biochim. Biophys. Acta 1248*, 81−96.
37. Jansonius, J. N. (1998) Structure, evolution and action of vitamin B_6-dependent enzymes, *Curr. Opin. Struct. Biol. 8*, 759−769.

BI035324P